Applied Physics Letters

Passive fine-tuning of microcavity whispering gallery mode for nonlinear optics by thermo-optical effect

Cite as: Appl. Phys. Lett. **114**, 101103 (2019); https://doi.org/10.1063/1.5085923
Submitted: 17 December 2018 . Accepted: 24 February 2019 . Published Online: 12 March 2019

Yaming Feng, Yuanlin Zheng, Fangxing Zhang, Jianfan Yang, Tian Qin, and Wenjie Wan

AIP Publishing

Applied Physics Letters ARTICLE scitation.org/journal/apl

Passive fine-tuning of microcavity whispering gallery mode for nonlinear optics by thermo-optical effect

Cite as: Appl. Phys. Lett. **114**, 101103 (2019); doi: 10.1063/1.5085923
Submitted: 17 December 2018 · Accepted: 24 February 2019 ·
Published Online: 12 March 2019

Yaming Feng,[1] Yuanlin Zheng,[2,3] Fangxing Zhang,[2] Jianfan Yang,[2] Tian Qin,[2] and Wenjie Wan[1,2,a)]

AFFILIATIONS

[1]The State Key Laboratory of Advanced Optical Communication Systems and Networks and Collaborative Innovation Center of IFSA, School of Physics and Astronomy, Shanghai Jiao Tong University, Shanghai 200240, China
[2]MOE Key Laboratory for Laser Plasmas, The University of Michigan-Shanghai Jiao Tong University Joint Institute, Shanghai Jiao Tong University, Shanghai 200240, China
[3]Department of Electrical and Systems Engineering, Washington University, St. Louis, Missouri 63130, USA

[a)]**Author to whom correspondence should be addressed:** wenjie.wan@sjtu.edu.cn

ABSTRACT

Whispering-gallery-mode (WGM) microcavities strongly enhance nonlinear optical processes like optical frequency comb (OFC), Raman scattering, and optomechanics, which nowadays enable cutting-edge applications in microwave synthesis, optical sensing spectroscopy, and integrated photonics. Yet, tunability of their resonances, mostly via coarse and complicated mechanisms through temperature, electrical, or mechanical means, still poses a major challenge for precision applications as above. Here, we introduce a passive scheme to finely tune resonances of WGMs at MHz precision with an external probe. Such a probe remotely transfers heat through a gap from an optical microcavity, effectively tuning its resonances by thermal-optic nonlinearity. Moreover, we explore this unique technique in microcavity nonlinear optics, demonstrating the generation of a tunable OFC and backward stimulated Brillouin scattering with variable beating frequencies. This technique addresses the core problem of WGM microcavity's fine-tuning, paving the way for important applications like spectroscopy and frequency synthesis.

Whispering-gallery-mode (WGM) micro-cavities have been intensively investigated in a wide range of areas for both fundamental physics and practical applications. The ultra-high quality (Q) factors and ultra-small mode volumes make WGM micro-cavities ideal platforms for ultra-sensitive optical sensing, strongly enhanced nonlinear optics, cavity QED, optomechanics, and micro-scale optical frequency combs (OFCs).[1–5] However, one major obstacle halting the practical implementations in these applications is the lack of tunability for fixed microstructures unlike their bigger-scale opponents, i.e., Fabry–Pérot cavities. For example, WGMs have to be finely tuned to closely match with atomic lines in cavity QED;[6] dual-comb spectroscopy requires precision scanning of optical comb lines;[7] tunable microwave generation from stimulated Brillouin scattering (SBS) enabled sources also poses a great demand for tunability.[8] Previously, various approaches have been demonstrated to tune WGM resonances mainly through thermal, mechanical, electrical, and optical means.[9–12] Active thermal tuning through the thermo-optic effect can be easily implemented for a wide tuning range. For example, a WGM shift of 160 pm can be achieved in a temperature change of 10 K for a silica microsphere.[13] Mechanically, compressing or stretching of micro-cavities by external piezo-electric components has been widely reported to even cover a whole free spectral range (FSR) tuning.[10,14] Besides, the On-chip carrier injection method for tuning and modulation, however, only works for specific semiconductors like silicon.[15] However, integration of these active tuning elements remains difficult.

Among the above methods, thermo-optic tuning of WGMs is one of the popular methods for the resonance tuning. Thermo-optic tuning based on electrical heating has exhibited a tuning rate higher than 85 GHz/V^2 over a 300 GHz range for microtoroids;[16] similarly, silicon photonic micro-disks can also be tuned by heating the graphene covered surface,[17] or through the micro-heater placed on the top of a micro-ring;[18] laser or optical induced heating can also be applied to thermal tuning, either through microcavities' intrinsic material absorption, e.g., by a CO_2 laser,[19] or by attaching special light

absorbers, nanoparticles to the surfaces[20,21] during light illumination. However, all the above methods have to rely on active external sources, i.e., electric, light, or heat and complex structures, which makes them inconvenient to implement.

Here, we demonstrate a passive mechanism to achieve extremely fine-tuning at the MHz level of WGM resonances through the thermal optical effect only using an external probe. The probe serves as a heat sink to dissipate absorbed heat from an optical microcavity, tuning its resonances by altering temperature inside. Such a heat transfer based tuning scheme highly depends on the gap spacing as well as probes' materials. We can achieve up to a 300 MHz spanning range at a MHz resolution by finely positioning a silica fiber probe within a distance of 500 μm. We also found out a better tuning efficiency by a metallic copper probe with a larger thermal conductance. Moreover, by applying this technique, we show that a tunable optical frequency comb with variable family comb lines can be generated, which is hard to achieve previously by laser pumping or detuning. In addition, we demonstrate a tunable microwave frequency source based on cavity-enabled backward stimulated Brillouin scattering by this tuning scheme. Unlike previous active methods, the current precise method is passive and heat-source free, and it should be generally applicable for microcavity based applications, opening an avenue for important applications like spectroscopy and frequency synthesis.

In a common thermal tuning WGM scheme, the thermal effect induces the temperature-dependent resonance frequency shift Δf from the refractive index n and the diameter D variations in a fused silica microsphere, as follows:[22]

$$\Delta f = -f_0\left(\frac{1}{n}\frac{dn}{dT} + \frac{1}{D}\frac{dD}{dT}\right)\Delta T, \tag{1}$$

where $f_0 = c/\lambda_0$ is the cold microcavity resonant frequency at $T_0 = 293.15$ K and $n = 1.46$ is the refractive index of fused silica for $\lambda_0 = 1550$ nm. $dn/ndT = 8.52 \times 10^{-6}\,\mathrm{K}^{-1}$ (Ref. 23) and $dD/DdT = 0.55 \times 10^{-6}\,\mathrm{K}^{-1}$ (Ref. 24) are the thermo-optic coefficient and thermal expansion coefficient, respectively. According to the two coefficients, the thermo-optic effect will dominate the WGM frequency shift induced by temperature changing for the silica microcavity[25,26] and the effect caused by thermal expansion is just 6.1%. The thermal decay time of the microcavity is about 40 ms measured by a pump-probe method.[27] It is much longer than the response times of refractive index change by the thermo-optical effect and the thermal expansion.[18] As the Cu tip approaches the microcavity, the decay time deceases to 10 ms with L = 5 μm. This means that the external probe will help to dissipate the heat of the microcavity and then accelerate the cooling process. This phenomenon can also be explained from the perspective of thermal conductivity. For a silica microsphere, the temperature change ΔT is caused by the absorption of the resonant optical power coupled into the microcavity such that the input heat Q_{in} will equal the outgoing heat flow, i.e., $K_{eff}\Delta T$ at thermal equilibrium

$$Q_{in} = K_{eff}\Delta T, \tag{2}$$

where K_{eff} [J/(s · K)] is the effective absolute thermal conductivity contributed from the surrounding air, microsphere's structure, and supporting pillar.[28,29] From this perspective, if we purposely alter K_{eff} of a microcavity by modifying its surrounding medium, structures, or even supporting pillars, we may achieve a passive method without additional heating sources to change the internal temperature of the microcavity, effectively tuning the resonances.

Figure 1 shows one possible way to tune such microcavity resonances by placing an external solid probe in the vicinity. K_{eff} then becomes adjustable when varying the gap distance L between the probe and the microcavity. As a result, the WGM resonances will shift according to the internal temperature detuning caused by K_{eff} changing at thermal equilibrium. Here, an ultrahigh Q ($\sim 10^7$) silica microsphere with a diameter of around 240 μm is evanescently coupled by a tapered fiber. In the meantime, a standard optical silica fiber probe (125 μm in diameter) is placed near the microsphere to induce the thermal disturbance. The gap distance L between the micro-cavity and the fiber tip is varied form 5 μm to 500 μm by a translational stage with a micro-meter resolution. A pump laser of 1550 nm wavelength (New Focus, TLB-6700) is swept around one WGM resonance with a frequency span of 2 GHz at a rate of 20 Hz. The entire experimental apparatus is housed in an air-tight, temperature/humidity-controlled chamber. The microcavity and the coupling setup are sealed in an acrylic box to decrease the disturbance caused by air flow. The humidity is fixed at 30% by a dehumidifier. The temperature is maintained at 20 °C by an air conditioner.

Figure 1(b) shows a typical resonance frequency shift with respect to the gap variation by tuning the fiber tip. The probe is scanned in the equatorial plane. This is a representative direction which can demonstrate the tuning process conveniently and explicitly. We observe up to repeatable 292 MHz tuning ranges with an input power of 90 μW during the gap variation from 5 μm to 500 μm. In fact, the efficiency of the frequency tuning varies with scanning different directions. For example, the maximum value of frequency tuning will decease to 251 MHz along the polar axis with $L = 5$ μm. The fiber tip above the

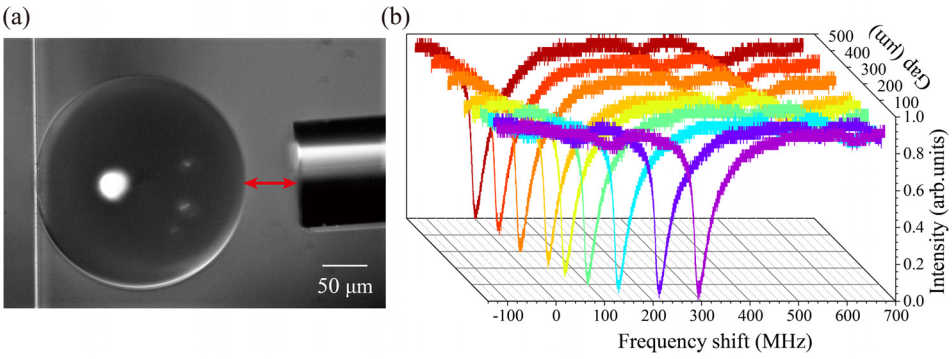

FIG. 1. The thermal fine-tuning apparatus and the related results. (a) Top view of the microcavity system. The gap distance L between the microsphere and the fiber probe is adjustable. (b) The WGM resonance frequency shift varies with the change in the gap distance L. A shift up to 300 MHz can be realized upon adjusting the gap around 500 μm.

polar point now is slightly further to the light mode's circulating orbit than that near the equatorial plane. Here, we achieve one easy and passive way to fine tune WGM resonances at a MHz resolution. Finer precision tuning, i.e., sub-MHz, can be obtained if the probe is positioned at a large distance using a nanometer-stage to control the gap distance.

Figure 2 shows the cause of such fine-tuning by considering heat transfer between the cavity and the probe. To model such a thermal tuning effect through gap varying, we perform finite element method (FEM) based heat transfer numerical simulations for comparison with experimental results.[30] The WGM involved here is a fundamental mode TE_{01}.The polarization of the electrical field is along the y axis. Here, the incoming heat flow Q_{in} results from the input optical power P_{in} through absorption with an effective mode area $A_{eff} = (\int\int E^2 dxdy)^2 / \int\int E^4 dxdy = 40.4\,\mu m^2$. The outgoing heat flows out of the cavity through the supporting pillar, the surrounded air, and the external probe nearby. The surrounding air has a specific thermal conductance of $K_{air} = 0.026\,W/(m \cdot K)$, far less than the materials we choose as the probe such as silica $K_{sio_2} = 1.38W/(m \cdot K)$ and copper $K_{cu} = 400W/(m \cdot K)$. Hence, the external probe serves as a good heat sink to transfer and dissipate the heat from the cavity. The gap spacing between them becomes very crucial to determine the whole system's effective absolute thermal conductivity $K_{eff}(L)$, which is hard to estimate analytically. Instead, for the given structure, we perform a FEM based numerical method to calculate the temperature change ΔT with respect to the gap varying and then compare them with our experiments through $\Delta f/\Delta T = -1.756\,GHz/K$ calculated using Eq. (1) in our experiment. In Fig. 2(a), for a silica fiber probe, ΔT varies almost linearly with a rate of $0.1\,mK/\mu m$ when $L > 200\,\mu m$, and then, it behaves approximately as $1/L$, reaching its maximum $\Delta T_{fiber-max} = -0.18\,K$ at $L = 5\,\mu m$. For a Cu probe, a similar trend can be observed while with a larger amplitude: the maximum ΔT_{Cu-max} is $-0.35\,K$ achieved at $L = 5\,\mu m$, proving the Cu probe as a better heat sink for its larger thermal conductivity. More insights can be obtained from the insets in Fig. 2(a) which show the temperature map of the microcavity system. Clearly, the Cu probe is warmer at a closer distance dissipating heat more efficiently. Indeed, the gap spacing plays a key role in dominating the heating transfer process in such micro-structures. Besides, the volume of the external probe can also affect the frequency tuning process. Three different Cu wires with diameters of $100\,\mu m$, $300\,\mu m$, and $1.81\,mm$ are tested, respectively. The corresponding maximum frequency shifts for the three wires are 292 MHz, 848 MHz, and 1296 MHz, respectively. It is obvious that the thicker the Cu wire is, the higher the tuning frequency shift will be obtained.

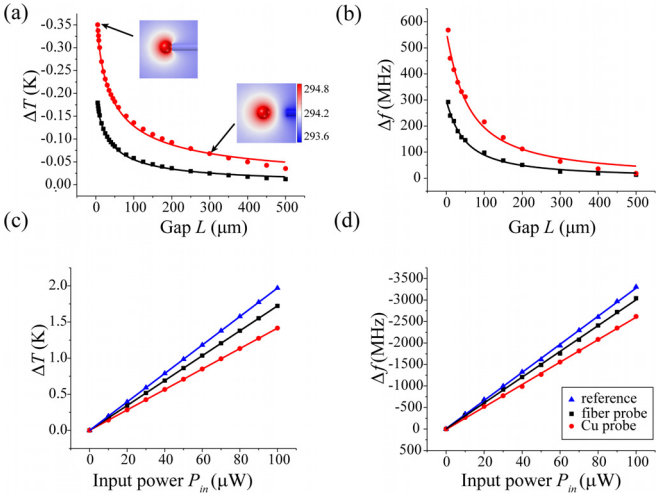

FIG. 2. The numerical simulations of temperature changes and the corresponding shift to frequency measured by the experiment. (a) The temperature change of microcavity ΔT varies with adjusting gap distance L. The insets show the temperature distribution of the microcavity system for the Cu probe with $L = 5\,\mu m$ and $300\,\mu m$. (b) The frequency shift Δf varies with gap L. The maximum values of Δf for the Cu probe are 568.10 MHz larger than that of the fiber probe 292.26 MHz at $L = 5\,\mu m$; even the diameter of the Cu probe $D_{cu} = 100\,\mu m$ is smaller than that of the fiber probe $D_{fiber} = 125\,\mu m$. (c) The temperature shift ΔT of the microcavity increases due to the increase in the input power P_{in}. The Cu probe is much effective in reducing ΔT than the fiber tip. The case of the fiber probe at $L = 800\,\mu m$ is also shown as a reference. The rates of the three lines (from up to down) are $19.69\,mK/\mu W$, $17.22\,mK/\mu W$, and $14.15\,mK/\mu W$, respectively. (d) The experimental data of the frequency shift Δf with the change in P_{in}. The rates of the three carves are $-33.04\,MHz/\mu W$, $-30.40\,MHz/\mu W$, and $-26.16\,MHz/\mu W$, respectively. The blue triangle, black square, and red circle lines present the reference fiber, fiber, and Cu probes, respectively. The solid lines are the fitting curves.

As a comparison, the experimental results in Fig. 2(b) exhibit similar trends for both silica and Cu probes. The average growing rates before $L = 100\,\mu m$ are $\eta_{fiber} = 0.21\,MHz/\mu m$ and $\eta_{cu} = 0.50\,MHz/\mu m$, respectively. At $L = 5\,\mu m$, the maximum frequency shifts are $\Delta f_{fiber} = 292.26\,MHz$ and $\Delta f_{cu} = 568.10\,MHz$, well matched with the above numerical calculations, i.e., $\Delta f_{fiber-sim} = 316.08\,MHz$ and $\Delta f_{Cu-sim} = 615.13\,MHz$. To further justify this thermal effect, the relationship between input power and ΔT has been examined with/without external probes. As shown in Figs. 2(c) and 2(d), the incoming heat causes an increase in temperature inside the cavity [from Eq. (2)], causing the shifts of resonances from Eq. (1). As a reference where the fiber probe is far away or absent, the temperature grows linearly with the input power at a rate of $19.69\,mK/\mu W$. When the probe is placed at $5\,\mu m$ away, the rate of temperature variation becomes smaller as $17.22\,mK/\mu W$ for the fiber probe and $14.15\,mK/\mu W$ for the copper probe. The corresponding frequency shift rates of the three lines are $-34.58\,MHz/\mu W$, $-30.24\,MHz/\mu W$, and $-24.85\,MHz/\mu W$, respectively. As a comparison, the measured frequency shift rates in our experiment in Fig. 2(d) are $-33.04\,MHz/\mu W$, $-30.40\,MHz/\mu W$, and $-26.16\,MHz/\mu W$, respectively. These results validate the thermal origin of such a fine-tuning mechanism in our microcavity system. As a proof of principle, two representative nonlinear optical applications will be shown below.

We will demonstrate tunable optical frequency comb (OFC) generation and backward stimulated Brillouin scattering (SBS) in the WGM micro-cavity now. Both the effects are of significance in fundamental science and realistic applications. The feasibility of a WGM based microcavity for fine tuning of frequency comb generation and backward SBS based on such a thermal effect is thus demonstrated. In our frequency comb generation, an intense input power (10 mW in our experiment) is injected into the microcavity. The experimental conditions are the same as the aforementioned experiment. The thermal locking is utilized to lock the laser frequency in the WGM resonance. The frequency comb generation in WGM micro-cavities is usually controlled by detuning the pump frequency. It should be noted that the laser frequency (1550.44 nm) is locked to a WGM resonance to generate the frequency comb throughout the tuning process. One

part of the output light from the microcavity is coupled into an optical spectrum analyzer (OSA) by a 50:50 fiber coupler. Thus, we can monitor the whole process while scanning the wavelength. During the experiment, the fiber tip is first placed in the vicinity of the microsphere, such as with a gap distance of 50 μm. The condition is found by slowly scanning (about 0.01 nm/s) the laser frequency until the frequency comb is generated. Then, the switching of different OFC families is realized by changing the gap distance between the microsphere and the fiber tip. As shown in Fig. 3, the fine tunability of the comb lines is obvious, which proves the feasibility of our scheme.

We also demonstrate the tunability of backward and forward SBS frequencies in the WGM micro-cavity. Backward SBS phenomena in WGM micro-resonators are the fundamental phenomena for ultra-narrow linewidth lasers close to quantum limits. The method we proposed may be useful in achieving finely tunable SBS lasers. The fundamental principles of generating backward/forward SBSs are illustrated in Figs. 4(a) and 4(b). For the backward SBS, the Stokes light is reflected back directly by the acoustic wave excited by electrostriction. According to momentum and energy conservation laws, the phase matching condition requires: $k_a = k_p + k_s$. The frequency of the acoustic wave $f_a = v_a/k_a$ is usually around ten GHz for the cavity made of silica. But for the forward SBS, the pump and Stokes light beams co-propagate in the same direction. The wave vector of the acoustic wave is now determined by $k_a = k_p - k_s$. The corresponding acoustic frequency is much smaller than that of back SBS. In the backward SBS experiment, the microsphere diameter is enlarged to approximately 700 μm (by fusing multiple times) to encourage the generation of SBS. The backward SBS occurs at two optical WGMs separated in frequency exactly by that of the phonon, which has a gain bandwidth of dozens of MHz.[31] They belong to different mode orders (different mode families). The induced frequency shift is therefore slightly different for the two modes. Hence, the variation of the frequency shift

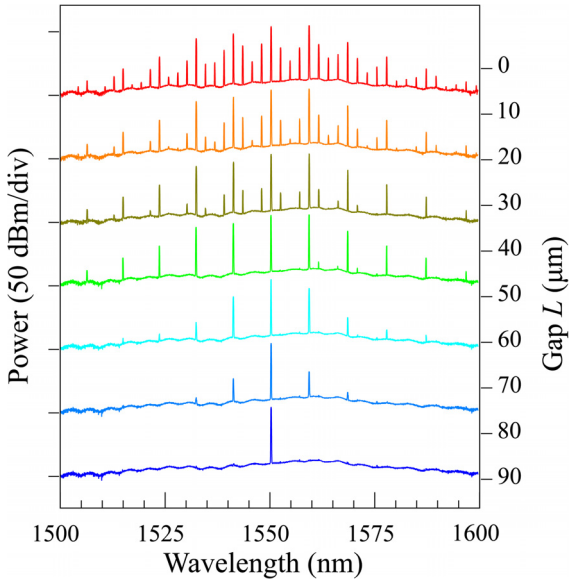

FIG. 3. Fine tuning of optical frequency comb generation. The evolution of the frequency comb generation spectrum as the fiber probe approaches the microsphere. Different OFC families can be chosen by adjusting the gap distance.

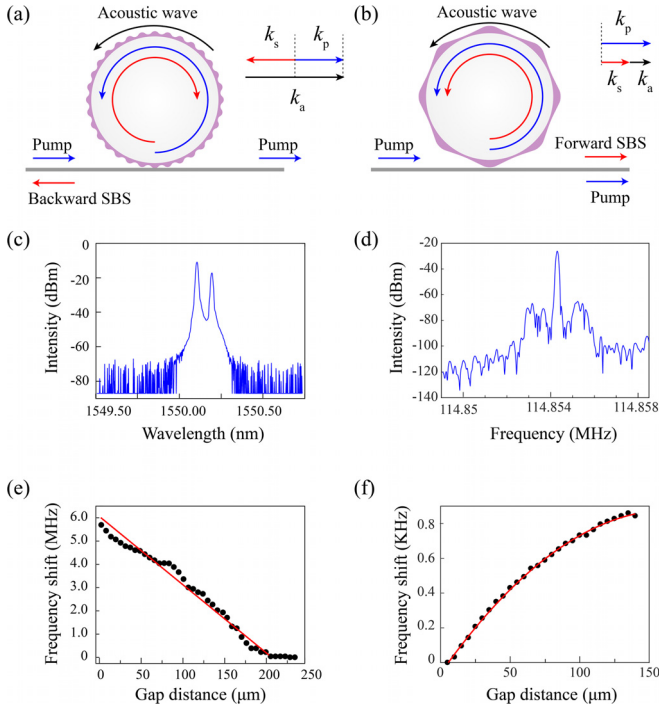

FIG. 4. Tuning the backward SBS and forward SBS in a WGM microcavity. (a) and (b) The illustrations of back/forward SBS processes excited by the pump light in the WGM microcavity. (c) The optical spectrum of the observed backward SBS light captured by an OSA. (d) The electrical spectrum of the beating signal between the observed forward SBS and the pump. The center frequency is near 114.854 MHz. (e) The central frequency of backward SBS varies almost linearly, while the fiber tip approaches the microsphere. (f) The central frequency of the forward SBS signal varies upon tuning the gap distance.

incurs a minute change in the SBS frequency. Figure 4(c) shows the spectrum of the observed first-order SBS with a pumping power of 5 mW. The spectral resolution is 0.01 nm. Careful control is made to ensure that higher orders of SBS are not excited by monitoring OSA. We couple the pump light into a WGM and make sure that the pump is thermal locked. Then, the pump frequency is tuned slowly in the resonance to excited one SBS light. An OSA is used to monitor the whole tuning process, and so, we can precisely control the number of SBS stokes light. A polarization controller (PC) will also be used to control the polarization of input light coupled into the cavity to achieve a larger coupling efficiency. An SBS frequency of 10.820 GHz is observed when the fiber tip is not introduced, which increases as the fiber tip approaches the microsphere. The SBS frequency shift shows a nearly linear dependence on the gap distance as shown in Fig. 4(c). A tuning span of SBS frequency of about 5.6 MHz is achieved in the experiment while changing the gap distance around 200 μm. Experimental tests have also been conducted at different resonances, showing different frequency shift spans. Spans from 2 to 10 MHz were most often observed using microspheres with radii from 250 to 700 μm. For the forward SBS, the wavelength space between the pump and Stokes is beyond the OSA resolution. Hence, an electrical spectrum analyzer (ESA) is used to monitor the beating signal between the pump and Stokes light as shown in Fig. 4(d). The microcavity here has

a diameter of 180 μm. The central frequency of the forward SBS is around 114.854 MHz. With the help of the external probe, the central frequency can be tuned 0.86 KHz while adjusting the gap distance around 140 μm.It is clear that the tuning range is smaller than that for backward SBS. This is because of the narrow linewidth of the surface acoustic wave during the forward SBS which requires a stricter phase matching condition.[32]

In conclusion, we have demonstrated a method for fine tuning of WGM frequency in silica microspheres, using the passive thermal dissipation. A mode frequency shift up to 300 MHz is obtained by the fiber probe tip with a MHz resolution. The tuning process is directly related to the gap distance and the materials of the probe tips. With the fine-tuning capability, optical frequency comb generation and backward/forward SBS in the micro-cavities can be precisely tuned. The scheme opens an avenue for micro-cavity applications in nonlinear optics.

The authors thank the National Key R&D Program of China (Grant Nos. 2016YFA0302500 and 2017YFA0303700), the Natural Science Foundation of China (Grant Nos. 11674228, 11304201, and 61475100), the National 1000-plan Program (Youth), the Shanghai Scientific Innovation Program (Grant No. 14JC1402900), and the Shanghai Scientific Innovation Program for International Collaboration (Grant No. 15220721400).

REFERENCES

[1]Y. Y. Zhi, X. C. Yu, Q. H. Gong, L. Yang, and Y. F. Xiao, Adv. Mater. **29**, 1604920 (2017).
[2]Q. F. Yang, X. Yi, K. Y. Yang, and K. J. Vahala, Nat. Photonics **11**, 560–564 (2017).
[3]A. Imamog, D. D. Awschalom, G. Burkard, D. P. DiVincenzo, D. Loss, M. Sherwin, and A. Small, Phys. Rev. Lett. **83**, 4204 (1999).
[4]M. Aspelmeyer, T. J. Kippenberg, and F. Marquardt, Rev. Mod. Phys. **86**, 1391–1452 (2014).
[5]X. Xue, Y. Xuan, Y. Liu, P.-H. Wang, S. Chen, J. Wang, D. E. Leaird, M. Qi, and A. M. Weiner, Nat. Photonics **9**, 594–600 (2015).
[6]W. von Klitzing, R. Long, V. S. Ilchenko, J. Hare, and V. Lefèvre-Seguin, "Frequency tuning of the whispering-gallery modes of silica microspheres for cavity quantum electrodynamics and spectroscopy," Opt. Lett. **26**, 166–168 (2001).
[7]A. Dutt, C. Joshi, X. Ji, J. Cardenas, Y. Okawachi, K. Luke, A. L. Gaeta, and M. Lipson, Sci. Adv. **4**, e1701858 (2018).
[8]C. Guo, K. Che, Z. Cai, S. Liu, G. Gu, C. Chu, P. Zhang, H. Fu, Z. Luo, and H. Xu, Opt. Lett. **40**(21), 4971–4974 (2015).
[9]B. Wild, R. Ferrini, R. Houdré, M. Mulot, S. Anand, and C. J. M. Smith, Appl. Phys. Lett. **84**, 846 (2004).
[10]K. N. Dinyari, R. J. Barbour, D. A. Golter, and H. Wang, Opt. Express **19**, 17966–17972 (2011).
[11]T. J. Wang, C. H. Chu, and C. Y. Lin, Opt. Lett. **32**, 2777–2779 (2007).
[12]S. Zhu, L. Shi, S. Yuan, X. Xu, and X. Zhang, Opt. Lett. **42**, 5133–5136 (2017).
[13]Q. Ma, T. Rossmann, and Z. Guo, J. Phys. D: Appl. Phys. **41**(24), 245111 (2008).
[14]M. Pöllinger, D. O'Shea, F. Warken, and A. Rauschenbeutel, Phys. Rev. Lett. **103**, 053901 (2009).
[15]Q. Xu, S. Manipatruni, B. Schmidt, J. Shakya, and M. Lipson, Opt. Express **15**, 430–436 (2007).
[16]D. Armani, B. Min, A. Martin, and K. J. Vahala, Appl. Phys. Lett. **85**(22), 5439–5441 (2004).
[17]L. Yu, Y. Yin, Y. Shi, D. Dai, and S. He, Optica **3**, 159–166 (2016).
[18]X. Xue, Y. Xuan, C. Wang, P.-H. Wang, Y. Liu, B. Niu, D. E. Leaird, M. Qi, and A. M. Weiner, Opt. Express **24**, 687–698 (2016).
[19]J. Zhu, S. K. Ozdemir, and L. Yang, Appl. Phys. Lett. **104**, 171114 (2014).
[20]K. D. Heylman, N. Thakkar, E. H. Horak, S. C. Quillin, C. Cherqui, K. A. Knapper, D. J. Masiello, and R. H. Goldsmith, Nat. Photonics **10**, 788–795 (2016).
[21]S. Zhu, L. Shi, B. Xiao, X. Zhang, and X. Fan, ACS Photonics **5**(9), 3794–3800 (2018).
[22]C. H. Dong, L. He, Y. F. Xiao, V. R. Gaddam, S. K. Ozdemir, Z. F. Han, G. C. Guo, and L. Yang, Appl. Phys. Lett. **94**, 231119 (2009).
[23]D. B. Leviton and B. J. Frey, Proc. SPIE **6273**, 62732 (2006).
[24]See http://accuratus.com/fused.html for "Fused Silica Engineering Properties" (last accessed December 15, 2018).
[25]J. Zhu, S. K. Ozdemir, L. He, and L. Yang, Appl. Phys. Lett. **99**, 171101 (2011).
[26]A. M. Armani, R. P. Kulkarni, S. E. Fraser, R. C. Flagan, and K. J. Vahala, Science **317**, 783–787 (2007).
[27]J. Wang, Y. Xuan, A. M. Weiner, and M. Qi, *Conference on Lasers and Electro-Optics (CLEO)* (IEEE, 2014), pp. 1–2.
[28]T. Carmon, L. Yang, and K. J. Vahala, Opt. Express **12**, 4742–4750 (2004).
[29]K. D. Heylman and R. H. Goldsmith, Appl. Phys. Lett. **103**, 211116 (2013).
[30]See https://www.comsol.com/products for "COMSOL Multiphysics®" (last accessed December 15, 2018).
[31]R. W. Boyd, *Nonlinear Optics* (Academic Press, Elsevier, 2008), p. 441.
[32]G. Bahl, J. Zehnpfennig, M. Tomes, and T. Carmon, Nat. Commun. **2**, 403 (2011).